The method of a floating frame of reference for non-smooth contact dynamics

Alexander Lozovskiy, Loïc Daridon, Frédéric Dubois, Stéphane Pagano

The method of a floating frame of reference for non-smooth contact dynamics

Alexander Lozovskiy, Loic Daridon, Frederic Dubois, Stephane Pagano

Laboratoire de Mécanique et Génie Civil (LMGC), Université Montpellier 2, CNRS, CC 048, Pl. E. Bataillon, 34095 Montpellier, France

Laboratoire de Micromécanique et d'Intégrité des Structures, MIST Laboratory, IRSN-CNRS-Université Montpellier 2, France

Abstract

A method of a floating frame of reference that performs splitting of a deformable solid into rigid and deforming parts is presented within the context of discrete element method. The decomposition is made in such a way that the deforming part of the velocity field does not contribute to the motion of the center of mass and to the rotational motion. The corresponding numerical method that computes both rigid and deforming motions is presented and extended to simulation of multi-body dynamics allowing non-smooth contact interactions, such as impacts and friction. Numerical experiments, where the method is compared with a more traditionally used Total Lagrangian method, justify its preference as a more efficient tool for the simulation of assemblies of stiff and massive objects.

Keywords: floating frame, velocity decomposition, discrete element method, non-smooth contact dynamics, multi-body dynamics

1. Introduction

This paper presents and studies the application of the method of a floating frame of reference for solids, participating in multi-body dynamics, simulated with the discrete element method.

The method of a floating frame of reference (for simplicity, it shall be called FFR) is a special type of a general family of so called corotational methods. The key idea of a corotational method is a kinematical splitting into two of the reference configuration of an element of a structure primarily discretized with the Finite Element method (FEM). These are the base configuration and the corotated, or dynamic one. The base configuration is kept fixed for the entire structural analysis, while the corotated configuration is a result of the rigid body motion, i.e. superposition of translation and rotation, of the base configuration. In general, the dynamic cofiguration is

Email addresses: alexander.lozovskiy@univ-montp2.fr (Alexander Lozovskiy), loic.daridon@univ-montp2.fr (Loic Daridon), frederic.dubois@univ-montp2.fr (Frederic Dubois), stephane.pagano@univ-montp2.fr (Stephane Pagano)

element dependent and is defined for each element separately. A far from complete list of the works on the topic includes [1]-[10].

The FFR method differes significantly from the general corotational methods by the fact that it requires only one dynamic configuration for each element. Even more, this single moving frame of reference is introduced without any connection with the elements or any other type of structural discretization of the described solid, and therefore it can be defined before even considering discretization in general. The FFR method is intuitively more attractive and has been known for over a century. It has been mostly used for computations in flexible multi-body dynamics, where separate solids are connected via bilateral constraints, typically smooth, [11], [12]. A brief overview of the method in this area was given in [13].

Our area of interest is the simulation of a large assemblies of bodies undergoing non-smooth contact interactions such as shocks and friction, with typically natural external forces such as gravity. The number of bodies ranges from hundreds to hundreds of thousands or even more. The bodies are assumed to fall under two important restrictions. One of the restrictions is that the bodies are seen as massive blocks, which means no extremely thin bodies are considered. The second restriction imposes large stiffness on the participating bodies, for which the Young modulus is typically positioned around minimum values of order $10^9 \sim 10^{10}$ or larger. These restrictions eliminate possibility of non-linear deformational behavior, such as bending. The areas of application of the discrete element method (DEM) with these assumptions include rocking avalanches [14], [15], masonry structures, granular systems. Even the most sophisticated continuous flow models usually fail to replace DEM in representing accurate physical phenomena.

This article focuses on the implementation of the FFR method for the discrete element method in multi-body dynamics and its integration into the non-smooth contact framework pioneered by J. J. Moreau [16],[17] and M. Jean [18]. This is a vastly growing field, and the number of methods has been developed for that framework. Unfortunately, the absolute rigidity model for interacting bodies in a studied collection as a simplification of a large stiffness model may create indeterminancy of solution, partly because of specific nature of employed interaction laws. One of the ways of treating this problem is introduction of finite yet large stiffness for the bodies, and therefore applying FEM analysis. This bears the most general solver relying on Total or Updated Lagrangian approach, also known in the engineering community as the method of large transformation. The method without any regard to contact is thoroughly described in [19] and its implementation into contact problems may be found in [20], [21]. With assumption of small rotation, the non-linearity of the method is neglected, and it is renamed into the method of small deformation.

Neither the corotational method, nor the large transformation approach seem as attractive for the non-smooth dynamics of stiff massive solids as the FFR method. Assuming the solid's position field satisfies $\mathbf{x} = \mathbf{F}(\mathbf{X})$ from the base configuration $\mathbf{X}$ to the current configuration $\mathbf{x}$, the transformation gradient may be polarly decomposed as

$$\frac{\partial \mathbf{F}}{\partial \mathbf{X}} = \mathbb{U}\mathbb{O},$$

where $\mathbb{U}$ is responsible for deformation, and $\mathbb{O}$ is an orientation as of rigid body. The assumption for our case implies $\mathbb{O} \approx const$ for the entire structure, therefore the general corotational method, operating with arbitrarily changing $\mathbb{O}$ from element to element, is overused. On the other side, the large transformation approach is not efficient computationally, due to presence of high non-linearity in the equations even in the absence of contact interactions. The floating frame is intended for tracking the rotational part of the solid, and the non-linear deformations in this

case are completely eliminated from the point of view of that frame, which allows for constant stiffness matrix in the computations throughout the whole simulation. The left non-linearity is only due to rotations, which relaxes an iterative solution process.

The other attractive property of the FFR method is that the floating frame, if chosen right, may provide such characteristics of the moving solid as its center of mass, orientation and angular velocity (without operating to rigid body modes, coming from the FEM discretization), which are parameters of a purely rigid body and are desirable for intuitive description of deformable, but very stiff solids.

The presented work is done within the framework of Saladyn project whose goal is to create software for the simulation of dynamics of mechanical systems assuming non-smooth behavior. One of the related works is [18].

The paper has 4 sections following. As a theoretical base, section 2 provides formal kinematical theory in case of a very general body structure. It is shown that the decomposition into the rigid and the deformational motions of a single body is always possible in the kinematical sense regardless of the dynamical reasoning for the motion. Although theoretically this splitting is possible for any kind of deforming solids, computationally it is only meaningful for the area of application mentioned above, as too much of deformation would create non-linearity and the FFR method would not retain its advantageous status over the method of large transformation. Note this section is not operating with any sorts of spatial discretizations of a solid and is based purely on fundamental mechanical laws. This section may present interest especially for theoretical mechanicians. Section 3 introduces FEM method in the local frame for dealing with the deformational behavior and derives a stable second-order accurate Newmark time-stepping scheme and then adapts these results to non-smooth contact dynamics of a multi-body system. Finally, Section 4 contains numerical experiments that test the performance and accuracy of the method compared to the large transformation method. Section 5 provides the conclusion and further prospects.

2. The formalism

Everywhere below any bold symbol, for example $\mathbf{a}$, describes a vector with at least two components or a set of vectors. Blackboard bold symbols, except for the real number set $\mathbb{R}$, denote operators, tensors(wider than vectors) and their corresponding matrices. Symbol $\times$ denotes vector product and $\otimes$ denotes tensor product of two vectors, i.e. $\mathbf{a} \otimes \mathbf{b} = \mathbf{a}\mathbf{b}^T$. Operation $\mathbb{A} : \mathbb{B}$ returns the sum of all products of the corresponding elements of both matrices, i.e. $\sum_{i,j} A_{ij}B_{ij}$.

2.1. Kinematics

Let the Euclidean system of coordinates $Oxyz$ be an inertial frame of reference called a global frame. For a solid with density ρ and mass m, let $\mathbf{x}(\mathbf{X}, t)$ denote a position vector in the global frame of a material point with Lagrange coordinates $\mathbf{X}$ at time t. $\mathbf{v}(\mathbf{X}, t)$ denotes the velocity vector of that point. The set of all $\mathbf{X}$ is denoted V.

The main idea behind a floating frame is that any motion of a deformable body V may be described as the superposition of the motions of the imaginary rigid and the imaginary deforming parts. For a currently used floating orthonormal frame $CXYZ$ and an imaginary rigid body frozen in it, its center of mass placed at the origin C, the velocity $\mathbf{v}_R$ of that rigid body is completely defined by the motion of the floating frame. With the deforming velocity denoted as $\mathbf{v}_D$, the actual velocity satisfies

$$\mathbf{v} = \mathbf{v}_R + \mathbf{v}_D. \tag{1}$$

So once a rigid part $\mathbf{x}_R(\mathbf{X}, t)$ and its corresponding floating frame, also called local or rigid frame, are specified in any desired way, the equality (1) uniquely defines $\mathbf{v}_D$ for a provided motion of the actual solid with velocity $\mathbf{v}$.

The orientation of $CXYZ$ is given by orthogonal matrix $\mathbb{O}(t)$. $\mathbf{r}(\mathbf{X}, t)$ denotes a vector, expressed in the global frame, from the center of mass of the rigid part to the point of the same with material coordinates $\mathbf{X}$. By definition of $\mathbb{O}$,

$$\mathbf{r}(\mathbf{X}, t) = \mathbb{O}(t)\mathbf{X}. \tag{2}$$

Let ρ_R denote density of the rigid part. For every rigid body moving continuously in space, there exists a two-way correspondence between $\mathbf{v}_R$ and the velocity of the center of mass $\mathbf{v}_{R,C}$ and its angular velocity $\boldsymbol{\omega}$. This correspondence is based on linear operators $\mathbb{L}$ and $\mathbb{G}$, acting from a vector field to a single vector and in the opposite direction respectively:

$$\mathbb{L} : \mathbf{v}_R \to \begin{pmatrix} \mathbf{v}_{R,C} \\ \boldsymbol{\omega} \end{pmatrix}, \mathbb{G} : \begin{pmatrix} \mathbf{v}_{R,C} \\ \boldsymbol{\omega} \end{pmatrix} \to \mathbf{v}_R.$$

With $\mathbb{J} = \int_V \rho_R((\mathbf{r}^T\mathbf{r})\mathbb{I} - \mathbf{r} \otimes \mathbf{r})dv$ denoting the inertia tensor of the rigid part *in the global axes* at the center of mass (so called Koenig's frame of reference) and being diagonal *in the local frame*, operator $\mathbb{L}$ has form

$$\mathbb{L} = \begin{pmatrix} m^{-1} \int_V \rho_R \cdot (\cdot)dv \\ \mathbb{J}^{-1} \int_V \rho_R \mathbf{r} \times (\cdot)dv \end{pmatrix}.$$

Note the Koenig's frame implies time-dependence of $\mathbb{J}$. $\mathbb{G}$ is simply another way of writing Euler's formula

$$\mathbf{v}_R = \mathbf{v}_{R,C} + \boldsymbol{\omega} \times \mathbf{r}. \tag{3}$$

It is obvious that $\mathbb{G}\mathbb{L}\mathbf{v}_R = \mathbf{v}_R$.

We are interested in condition

$$\mathbb{L}\mathbf{v}_D = 0. \tag{4}$$

Theorem 1. *For every continuously moving body, there always exists such a decomposition into the rigid and the deforming parts that* $\mathbb{L}\mathbf{v}_D = 0$ *for the whole motion of the body. The decomposition is unique, up to initial configuration of the rigid part.*

Proof.

Indeed, specify rigid part in any desired way at the initial moment $t = 0$ (only preserving isomorphism between $\mathbf{x}$ and $\mathbf{x}_R$). Its velocity is defined via $\mathbf{v}_R = \mathbf{v}_{R,C} + \boldsymbol{\omega} \times \mathbf{r}$. Since field $\mathbf{r}$ is fixed (it defines the rigid part that we constructed), we only need to adjust two vectors $\mathbf{v}_{R,C}$ and $\boldsymbol{\omega}$ in the way we like. Setting

$$\mathbf{v}_{R,C} = m^{-1} \int_V \rho_R \mathbf{v} dv, \tag{5}$$

$$\boldsymbol{\omega} = \mathbb{J}^{-1} \int_V \mathbf{r} \times \rho_R \mathbf{v} dv. \tag{6}$$

immediately satisfies (4). If at the initial time we set the rigid velocity in the way described above, this decomposition will preserve condition (4) for the whole motion if we simply force conditions (5) and (6) for the rigid part satisfied. ■

Remark 1. *The theorem may also be proven with use of the fact that set* $\mathbf{V}$ *of all fields* $\mathbf{v}$ *for a fixed moment of time is a Hilbert space with inner product* $\langle \cdot, \cdot \rangle = \int_V \rho_R(\cdot)^T(\cdot)dv$. *The set* $\mathbf{V}_R = \{\mathbf{v}_R | \mathbf{v}_R = \mathbf{v}_{R,C} + \boldsymbol{\omega} \times \mathbf{r}\}$, *parametrized by* $\mathbf{v}_{R,C}$ *and* $\boldsymbol{\omega}$, *is a linear subspace of* $\mathbf{V}$ *and* $\mathbb{GL}$ *is a projection operator from* $\mathbf{V}$ *onto* $\mathbf{V}_R$. *By properties of Hilbert space, there exists a unique element* $\mathbf{v}_R \in \mathbf{V}_R$ *such that* $\mathbb{GL}(\mathbf{v} - \mathbf{v}_R) = 0$, *i.e.* $\mathbb{L}\mathbf{v}_D = 0$, *since Ker*$\mathbb{G} = 0$.

Starting now, for each solid we shall consider such a rigid part from an infinite set of those satisfying (4), that the center of mass of the rigid part coincides with that of the actual body and the internal forces arising from deformations are reduced to zero. Physically, condition (4) implies that the bulk behavior preserves the motion of the center of mass of the whole system and its rotational momentum. $\mathbf{v}_{R,C}$ is naturally replaced with $\mathbf{v}_C$, for simpler notation. Due to (1) and (4),

$$\mathbb{GL}\mathbf{v} = \mathbf{v}_R \text{ and } (\mathbb{I} - \mathbb{GL})\mathbf{v} = \mathbf{v}_D.$$

The following holds.

Proposition 1.

$$\int_V \rho_R \mathbf{v}_R^T \mathbf{v}_D dv = 0. \tag{7}$$

Proof. The statement of the proposition is obtained immediately by applying the argument of Remark 1. ■

Remark 2. *Theorem 1 lets decompose the total kinetic energy of the system into the kinetic energy of the rigid motion and of the deforming one.*

$$T = \frac{1}{2}\boldsymbol{\omega}^T \mathbb{J}\boldsymbol{\omega} + \frac{1}{2}mv_C^2 + \frac{1}{2}\int_V \rho_R \mathbf{v}_D^T \mathbf{v}_D dv.$$

Coordinate function $\mathbf{x}'(\mathbf{X}, t)$ describes the actual motion of the points of the body with respect to frame $CXYZ$ (local, or relative motion). The set of all $\mathbf{x}'(\mathbf{X})$ is denoted V'. With local velocity $\mathbf{v}' = \dot{\mathbf{x}}'$, the Galilean addition of velocities in the global frame reads as

$$\mathbf{v} = \mathbf{v}_C + \mathbb{O}\mathbf{v}' + \boldsymbol{\omega} \times \mathbb{O}\mathbf{x}'. \tag{8}$$

From here, it follows that

$$\mathbf{v}_D = \mathbb{O}(\mathbf{v}' + \mathbb{O}^T\boldsymbol{\omega} \times \mathbf{d}') \tag{9}$$

in the global frame with local displacement $\mathbf{d}' = \mathbf{x}' - \mathbf{X}$.

An interesting fact about presented decomposition is that for systems with small stiffness it provides a rigid frame, which intuitively does not seem obvious. Consider for instance a discrete system made of 4 equal mass points placed at the corners of a square and connected with each other through springs of equal stiffness. A simple algebraic calculation shows that if an initial rotation is imposed around the center of the square in the plane of the square and the points are left for free motion, the rigid frame does not have its axes passing through the points. There would be a time-dependent angle between the rigid frame and the one with the same origin, but constantly passing through the points, see Fig. 1. The components of the point-wise deforming velocity vector $\mathbf{v}_D$ are parallel to axes of CXY instead of $C\bar{X}\bar{Y}$. The angle between two frames α and, therefore, the drift get smaller if the stiffness increases, and reaches zero for absolutely rigid connections between the points. For the applications that this works aims at, the stiffness

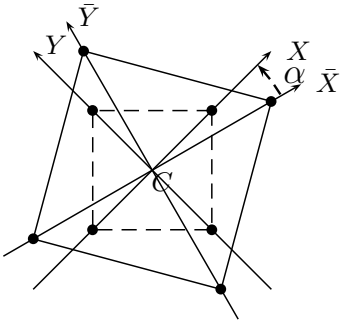

Figure 1: The system itself (outer square) and its rigid component (inner square)

is large enough for this kind of drift to remain unnoticed. The deforming velocity $\mathbf{v}_D$ may be unharmfully treated as $\mathbb{O}\mathbf{v}'$.

The absence of rotations with respect to the local frame provided by condition (4) is the main advantage of this frame compared to many others, since it allows to study material deformations in this frame without involving geometrical non-linearities.

2.2. Dynamics

The force vectors acting on a body are described as internal, i.e. those acting from the points of the body itself, and external forces. They are denoted $\mathbf{F}_{int}$ and $\mathbf{F}_{ext}$ respectively. Note that $\mathbf{F}_{ext}$ is considered here general space-independent volumic force, but material coordinate dependent. It is different from forces $\mathbf{R}$ acting on the surface, such as contacts.

Now we can write the main dynamics equation governing the solid pointwise:

$$\rho\dot{\mathbf{v}} = \mathbf{F}_{int} + \mathbf{F}_{ext} + \mathbf{R}, \tag{10}$$

where $\mathbf{R}$ is taken zero everywhere outside the contact region. The trajectory of the center of mass of the whole system is described via

$$\dot{\mathbf{v}}_C = \frac{1}{m}\left(\int_{V'} \mathbf{F}_{ext} dv' + \int_{\partial V'} \mathbf{R} ds\right), \tag{11}$$

which is a known result. Also, according to (6), the rotational motion of the system is determined via

$$\mathbb{J}\boldsymbol{\omega} = \int_{V'} \mathbb{O}\mathbf{X} \times \rho\mathbf{v} dv'. \tag{12}$$

Implicit time discretization of this equation creates an unstable scheme, and it additionally puts computational burden on the simulation, which comes from the need of integration over the entire solid. Instead, (12) must be differentiated in time. This provides an equation, which is too heavy for practical computations, and all the terms of order higher than zero with respect to the deformational (bulk) degrees of freedom are dropped. So we obtain the equation of angular momentum for a purely rigid body:

$$(\dot{\mathbb{J}\boldsymbol{\omega}}) = \int_{V} \mathbb{O}\mathbf{X} \times \mathbf{F}_{ext} dv + \int_{\partial V'} \mathbb{O}\mathbf{X} \times \mathbf{R} ds \tag{13}$$

This drastic simplification is justified by the fact of small perturbation allowed for the solid. Numerical tests will show satisfactory results for this simplified equation within our framework of assemblies of very stiff objects. For interested readers, the equation with one order higher, i.e. linearized, is derived in Appendix A.

We can now write dynamics formulation for the deforming motion. Recall that consideration of dynamics in the local frame, as opposed to the global one, introduces *fictitious forces*. Denote by $\tilde{\boldsymbol{\omega}} = \mathbb{O}^T\boldsymbol{\omega}$, $\tilde{\dot{\boldsymbol{\omega}}} = \mathbb{O}^T\dot{\boldsymbol{\omega}}$ the standard geometrical vector transformations from the global frame to the local one and $\tilde{\mathbb{T}} = \mathbb{O}^T\mathbb{T}\mathbb{O}$ denotes the Cauchy stress tensor in the rigid frame of reference. Then the momentum equation in the local frame is

$$\rho\dot{\mathbf{v}}^{'} = \nabla\cdot\tilde{\mathbb{T}} + \mathbb{O}^T\mathbf{F}_{ext} + \mathbf{F}_{tr} + \mathbf{F}_{rot}, \tag{14}$$

where

$$\mathbf{F}_{tr} = -\mathbb{O}^T\rho\dot{\mathbf{v}}_C,$$

$$\mathbf{F}_{rot} = -\tilde{\boldsymbol{\omega}}\times(\tilde{\boldsymbol{\omega}}\times\rho\mathbf{x}^{'}) - \tilde{\dot{\boldsymbol{\omega}}}\times\rho\mathbf{x}^{'} - 2\tilde{\boldsymbol{\omega}}\times\rho\mathbf{v}^{'}.$$

Term $\mathbf{F}_{tr}$ is a translational inertia force and distributed homogeneously over the whole solid, acting as an additional gravity pointing in the direction opposite to the solid's translational acceleration. In computations, this term is better written in terms of external forces and contact due to (11). Term $\mathbf{F}_{rot}$ consists of rotational fictitious forces, namely, the centrifugal, Euler and Coriolis forces.

Note that equations (11) and (12) require only time discretization, while equation (14) is the one requiring both temporal and FEM discretization. The latter one provides the most computational load. In this paper, elasticity law $\mathbb{T} = \mathbb{C} : \mathbb{E}$ with strain tensor $\mathbb{E}$ is imposed on the stress tensor since the deformations are assumed to be small. The nonlinear with respect to displacement and velocity terms are neglected. This lets us use time-independent volume V and its surface ∂V instead of $V^{'}$ and $\partial V^{'}$ in various integrations employed in Finite Element discretization. We should obtain standard formulation of elastic problem with constant in time stiffness matrix.

As we have finished with the formalism, it is now possible to construct a consistent numerical method for solving (10) using the FFR method.

3. The numerical method

If a rigid state of a body is provided at the initial moment of time, then it gives unique operators $\mathbb{L}$ and $\mathbb{G}$ for it, so this allows to find $\mathbf{v}_R = \mathbb{G}\mathbb{L}\mathbf{v}$ and, consequently, $\mathbf{v}_D$. From it, we easily obtain $\mathbf{v}^{'}$ using (9). The time-step is denoted h and is assumed constant in this paper. The value of discrete function f at the node i, corresponding to $t_i = t_0 + hi$, is denoted f_i.

3.1. Single solid

Traditionally, in non-smooth contact dynamics (NSCD) all the contact interactions are represented as those occuring through finite set of points rather than continuum surfaces, as the last case lacks consistent general framework due to its difficulty. The non smooth contact framework relies on so called contact laws that are written for each point individually, together organizing a contact network with a global contact law. A commonly used one and employed in this paper is the law connecting the reaction at the current contact point $\mathbf{R}$ with the relative velocity of the

interacting solids at that point **U**, for example, Signorini non-penetration condition and Coulomb friction law with friction coefficient μ, respectively below:

$$\begin{cases} R_N = proj_{\mathbb{R}_+}(R_N - c_N g), \\ \mathbf{R}_T = proj_{D(\mu R_N)}(\mathbf{R}_T - c_T \mathbf{U}_T). \end{cases}$$

Here subscripts N and T mean normal and tangential components respectively, $g \geqslant 0$ is the gap function, c means positive conditioning coefficient, and $D(r)$ means a two-dimesional disk of radius r. For more on this, as well as more used Signorini velocity condition, see [16]-[18], [22].

For practical purposes, at least for one body in contact, a contact point that this structure is having at a certain moment of time is assumed to be precisely a node of the mesh arising from its space discretization, such as Finite Element discretization. Then for the second body, since the actual contact region in general is not localised close enough to either of the FEM nodes on its surface, the position of its contact point is found from orthogonal projection of the point of the first body to the surface of the second.

Let the body have a set $\{\alpha\}$ of contact points on its surface over the time interval $[t_i, t_{i+1}]$. There is an orientation at contact point α given via matrix $\mathbb{C}_\alpha$ that is constructed from its basis vector being orthogonal to the surface of the body at the contact point. So we assume by default that at least one of the bodies has a smooth (in geometrical sense) surface at the contact point during the contact in order for $\mathbb{C}_\alpha$ to be defined correctly. Reaction at point α expressed in $\mathbb{C}_\alpha$ is denoted $\tilde{\mathbf{R}}_\alpha$. So in the global frame $\mathbf{R}_\alpha = \mathbb{C}_\alpha \tilde{\mathbf{R}}_\alpha$. Note that in general $\mathbb{C}_\alpha \neq \mathbb{O}$. There is also a strong assumption that the contact geometry does not change during time interval $[t_i, t_{i+1}]$, which is equivalent to the fact that $\mathbb{C}_\alpha$ remains constant over the interval and point α does not move in the local frame. Nevertheless, to achive as much generality as possible, we assume that $\mathbb{O}$ may be changing over time interval $[t_i, t_{i+1}]$. This may happen, for example, when body turns while touching a static surface with its corner.

We shall consequtively discretize (11), (13) and (14). The scheme used for temporal discretization is a Newmark symmetric one (also called trapezoidal), known for being a second-order accurate, unconditionally stable implicit scheme, [23], [24]. For (11), obtain

$$\mathbf{v}_{C,i+1} = \mathbf{v}_{C,i} + \frac{h}{2m} \int_V (\mathbf{F}_{ext,i} + \mathbf{F}_{ext,i+1}) dv + \frac{h}{m} \sum_\alpha \mathbb{C}_\alpha \tilde{\mathbf{R}}_\alpha. \tag{15}$$

For the rotational motion (13), obtain

$$\begin{aligned} \mathbb{J}_{i+1} \boldsymbol{\omega}_{i+1} = \mathbb{J}_i \boldsymbol{\omega}_i &+ \frac{h}{2} \int_V \mathbb{O}_i \mathbf{X} \times \mathbf{F}_{ext,i} dv + \frac{h}{2} \int_V \mathbb{O}_{i+1} \mathbf{X} \times \mathbf{F}_{ext,i+1} dv \\ &+ h \mathbb{O}_{i+1} \sum_\alpha \mathbf{X}(\alpha) \times \mathbb{O}_{i+1}^T \mathbb{C}_\alpha \tilde{\mathbf{R}}_\alpha. \end{aligned} \tag{16}$$

Write the time-stepping equation for the deforming motion (14) as

$$\begin{aligned} \rho \mathbf{v}_{i+1}^{'} = \rho \mathbf{v}_i^{'} &+ \frac{h}{2} (\nabla \cdot \tilde{\mathbb{T}}_i + \nabla \cdot \tilde{\mathbb{T}}_{i+1}) + \frac{h}{2} (\mathbb{O}_i^T \mathbf{F}_{ext,i} + \mathbb{O}_{i+1}^T \mathbf{F}_{ext,i+1}) \\ &- \frac{h}{2} \frac{\rho}{m} \int_V (\mathbb{O}_i^T \mathbf{F}_{ext,i} + \mathbb{O}_{i+1}^T \mathbf{F}_{ext,i+1}) dv - h \frac{\rho}{m} \mathbb{O}_{i+1}^T \sum_\alpha \mathbb{C}_\alpha \tilde{\mathbf{R}}_\alpha + \frac{h}{2} (\mathbf{F}_{rot,i} + \mathbf{F}_{rot,i+1}). \end{aligned} \tag{17}$$

The two terms with integration and summation are the inertia force $\mathbf{F}_{tr}$ due to translation, expressed through the external and contact forces respectively. An interesting observation about a

typical structure we consider is that a small scale of its perturbation makes it possible to *neglect* the contribution of local displacement $\mathbf{d}'$ and its velocity $\mathbf{v}'$ in all three terms inside $\mathbf{F}_{rot}$, leaving only the influence coming from rigid configuration $\mathbf{X}$. This in particular completely eliminates Corilois term and leaves

$$\mathbf{F}_{rot} \approx -\tilde{\boldsymbol{\omega}} \times (\tilde{\boldsymbol{\omega}} \times \rho\mathbf{X}) - \tilde{\dot{\boldsymbol{\omega}}} \times \rho\mathbf{X}. \tag{18}$$

This is a very crucial advantage of the FFR method for very stiff objects, since FEM does not only create a constant in time stiffness matrix in this case, but also a constant mass matrix, so the inversion of a generalized matrix (see below) is simplified significantly. This makes it different from the applications of flexible multi-body dynamics, described in [13]. Note that for the centrifugal force its trapezoidal discretization is obviously taken as the average between two endpoints of the interval $[t_i, t_{i+1}]$ as opposed to Euler force, which is approximated as the mid-point due to impossibility to approximate the angular accelration at the endpoints:

$$-h\tilde{\dot{\boldsymbol{\omega}}} \times \rho\mathbf{X} \approx -\rho(\mathbb{O}_{i+1}^T \boldsymbol{\omega}_{i+1} - \mathbb{O}_i^T \boldsymbol{\omega}_i) \times \mathbf{X}.$$

Let $\{\boldsymbol{\phi}_j\}$ with $j = 1, \ldots, n$ denote the set of the basis nodal functions for the whatever Finite Element discretization we are using inside local frame $CXYZ$, and local displacement $\mathbf{d}'$ and velocity $\mathbf{v}'$ are approximated as $\sum_j \psi_j \boldsymbol{\phi}_j$ and $\sum_j \lambda_j \boldsymbol{\phi}_j$ respectively, with n unknowns ψ_j and $\lambda_j = \dot{\psi}_j$. So (17) bears its FEM analogue with mass matrix $\mathbb{M}$ and stiffness matrix $\mathbb{K}$ as

$$\begin{aligned}\left(\mathbb{M} + \frac{h^2}{4}\mathbb{K}\right)\boldsymbol{\lambda}_{i+1} &= \left(\mathbb{M} - \frac{h^2}{4}\mathbb{K}\right)\boldsymbol{\lambda}_i - h\mathbb{K}\boldsymbol{\psi}_i + \frac{h}{2}((\mathbf{F}_e)_i + (\mathbf{F}_e)_{i+1}) \\ &+ h\mathbf{A} + \mathbb{A}(\mathbb{O}_i^T \boldsymbol{\omega}_i - \mathbb{O}_{i+1}^T \boldsymbol{\omega}_{i+1}) + h\sum_\alpha \bar{\mathbb{H}}_\alpha^T \mathbb{O}_{i+1}^T \mathbb{C}_\alpha \tilde{\mathbf{R}}_\alpha.\end{aligned} \tag{19}$$

Here

$$\mathbb{A} = \int_V \rho_R \left(\mathbf{X} \times \boldsymbol{\phi}_1, \quad \mathbf{X} \times \boldsymbol{\phi}_2, \quad \cdots, \quad \mathbf{X} \times \boldsymbol{\phi}_n\right)^T dv,$$

$$\mathbf{A} = \int_V \rho_R \left(\boldsymbol{\phi}_1 \otimes \mathbf{X} : \mathbb{S} + s\mathbf{X}^T\boldsymbol{\phi}_1, \quad \boldsymbol{\phi}_2 \otimes \mathbf{X} : \mathbb{S} + s\mathbf{X}^T\boldsymbol{\phi}_2, \quad \cdots, \quad \boldsymbol{\phi}_n \otimes \mathbf{X} : \mathbb{S} + s\mathbf{X}^T\boldsymbol{\phi}_n\right)^T dv,$$

$$\mathbb{S} = -\frac{1}{2}\left(\mathbb{O}_i^T \boldsymbol{\omega}_i \otimes \boldsymbol{\omega}_i \mathbb{O}_i + \mathbb{O}_{i+1}^T \boldsymbol{\omega}_{i+1} \otimes \boldsymbol{\omega}_{i+1} \mathbb{O}_{i+1}\right),$$

$$s = \frac{1}{2}\left(|\boldsymbol{\omega}_i|^2 + |\boldsymbol{\omega}_{i+1}|^2\right).$$

Term $\mathbf{F}_e$ accounts for both the point-wise external force and its contribution inside $\mathbf{F}_{tr}$. Its j-th component is

$$\mathbf{F}_{e,j} = \mathbb{O}^T : \left(\int_V \boldsymbol{\phi}_j \otimes \mathbf{F}_{ext} dv - \frac{1}{m}\int_V \rho_R \boldsymbol{\phi}_j dv \otimes \int_V \mathbf{F}_{ext} dv\right).$$

$\mathbf{F}_e = 0$ for homogeneous in space external force, such as, for example, gravity. Similar to the external forces, the point-wise contact force and its contribution to the translational inertia term $\mathbf{F}_{tr}$ are organized together, via matrix $\bar{\mathbb{H}}_\alpha$ given as

$$\bar{\mathbb{H}}_\alpha = \left(\boldsymbol{\phi}_1(\alpha) - \tfrac{1}{m}\textstyle\int_V \rho_R \boldsymbol{\phi}_1 dv, \quad \boldsymbol{\phi}_2(\alpha) - \tfrac{1}{m}\textstyle\int_V \rho_R \boldsymbol{\phi}_2 dv, \quad \cdots, \quad \boldsymbol{\phi}_n(\alpha) - \tfrac{1}{m}\textstyle\int_V \rho_R \boldsymbol{\phi}_n dv\right). \tag{20}$$

The non-smooth contact dynamics framework connects the local degrees of freedom, for which the dynamics equations are formulated, with the actual ones, used for the formulation of physical

interaction laws between the solids. For the dynamics equations, two generalized mass matrices, explicit and implicit, uniting both the rigid and the deformational parts are introduced:

$$\mathbb{M}_{\pm} = \begin{pmatrix} m\mathbb{I}_{3\times 3} & 0 & 0 \\ 0 & \mathbb{J}_{i+\frac{1}{2}\pm\frac{1}{2}} & 0 \\ 0 & 0 & \mathbb{M} \pm \frac{h^2}{4}\mathbb{K} \end{pmatrix}.$$

In order to further integrate the presented FFR method into the NSCD framework, the evaluation of relative velocity $\mathbf{U}_\alpha$ in contact frame $\mathbb{C}_\alpha$ must be presented through local variables $\mathbf{v}_C$, $\boldsymbol{\omega}$, $\boldsymbol{\lambda}$. This evaluation is given by (8):

$$\mathbb{C}_\alpha \mathbf{U}_\alpha = \mathbf{v}_C + \boldsymbol{\omega} \times \mathbb{O}\mathbf{X}(\alpha) + \mathbb{O}\mathbf{v}'(\alpha) + \boldsymbol{\omega} \times \mathbb{O}\mathbf{d}'(\alpha).$$

The last term is non-linear with respect to the local variables, since local displacement $\mathbf{d}'_{i+1}$ is implicitly predicted through $\boldsymbol{\lambda}_{i+1}$. In this article, it is *dropped* even for large rotations, due to small deformability assumption. Nevertheless, the third term is kept regardless of it, as it is needed for treating the contact interactions with more degrees of freedom than in a case with purely rigid bodies. The numerical tests with neglected non-linear term show physically consistent results for moderate rotations, as they will be compared with the method of large transformation. So we shall obtain extended to rigid part matrices $\mathbb{H}_{\alpha\pm}$ so that explicit and implicit relative velocities are

$$(\mathbf{U}_\alpha)_{i+\frac{1}{2}\pm\frac{1}{2}} = \mathbb{H}_{\alpha\pm} \begin{pmatrix} \mathbf{v}_C \\ \boldsymbol{\omega} \\ \boldsymbol{\lambda} \end{pmatrix}_{i+\frac{1}{2}\pm\frac{1}{2}} \tag{21}$$

with hybrid term

$$\mathbb{H}_{\alpha\pm} = \mathbb{C}_\alpha^T \mathbb{O}_{i+\frac{1}{2}\pm\frac{1}{2}} \left(\mathbb{O}^T_{i+\frac{1}{2}\pm\frac{1}{2}}, \quad -\mathbb{X}(\alpha)\mathbb{O}^T_{i+\frac{1}{2}\pm\frac{1}{2}}, \quad \bar{\mathbb{H}}_\alpha \right). \tag{22}$$

Here $\mathbb{X}$ represents a skew-symmetric matrix for vector $\mathbf{X}$.

Remark 3. *Rigorously speaking, term $\bar{\mathbb{H}}_\alpha$ inside $\mathbb{H}_{\alpha\pm}$ defined by* (20) *should not contain inertia part (the integral terms in* (20)*) which is only used for correct distribution of the translational inertia force, arising from the reaction, over the whole FEM variables. In* (21)*, this part produces $\int_V \rho_R \sum_j \lambda_j \mathbf{u}_j dv$ which is a FEM approximation of $\int_V \rho_R \mathbf{v}' dv$, but since $\mathbf{v}_D$ is treated as $\mathbb{O}\mathbf{v}'$, according to section 2.1, this term may be seen as zero due to $\mathbb{L}\mathbf{v}_D = 0$.*

So the motion of a single body is formalized by a non-linear system of equations

$$\mathbb{M}_+ \begin{pmatrix} \mathbf{v}_C \\ \boldsymbol{\omega} \\ \boldsymbol{\lambda} \end{pmatrix}_{i+1} = \mathbb{M}_- \begin{pmatrix} \mathbf{v}_C \\ \boldsymbol{\omega} \\ \boldsymbol{\lambda} \end{pmatrix}_i + h\mathbf{F}_g + h \sum_\alpha \mathbb{H}^T_{\alpha+} \tilde{\mathbf{R}}_\alpha \tag{23}$$

with vector $\mathbf{F}_g$ containing the remaining non-contact terms of (15), (16) and (19) respectively. For the position variables, we shall have trapezoidal approximations in form

$$\mathbf{x}_{C,i+1} = \mathbf{x}_{C,i} + \frac{h}{2}(\mathbf{v}_{C,i} + \mathbf{v}_{C,i+1}),$$

$$\boldsymbol{\psi}_{i+1} = \boldsymbol{\psi}_i + \frac{h}{2}(\boldsymbol{\lambda}_i + \boldsymbol{\lambda}_{i+1}).$$

Let $\mathbb{Q}$ denote a skew-symmetric matrix of the angular velocity:

$$\mathbb{Q} = \begin{pmatrix} 0 & -\omega_z & \omega_y \\ \omega_z & 0 & -\omega_y \\ -\omega_y & \omega_x & 0 \end{pmatrix}.$$

From discretizing $\dot{\mathbb{O}} = \mathbb{Q}\mathbb{O}$, [11], we get

$$\mathbb{O}_{i+1} = \left(\mathbb{I} - \frac{h}{2}\mathbb{Q}_{i+1}\right)^{-1}\left(\mathbb{I} + \frac{h}{2}\mathbb{Q}_i\right)\mathbb{O}_i. \tag{24}$$

3.2. Multi-body system with contact

If all $\tilde{\mathbf{R}}_\alpha$ in (23) were known, this system of $6 + n$ equations for each time step could be solved with some iterative solver for non-linear systems. The information about $\tilde{\mathbf{R}}_\alpha$ can only be obtained via coupling with interaction laws, arising in non-smooth multi-body dynamics. Consider a system of N bodies, and for each body an algorithm (23) is used. Let $0.5 \leqslant \theta \leqslant 1$. Uniting dynamics equations together with the connection between generalized velocities and the actual relative velocities at contacts, we obtain the global system for multi-body dynamics

$$\begin{pmatrix} \mathbb{M}_+ & -h\mathbb{H}_+^T \\ \theta\mathbb{H}_+ & 0 \end{pmatrix} \cdot \begin{pmatrix} \mathbf{V}_{i+1} \\ \mathbf{R} \end{pmatrix} = \begin{pmatrix} \mathbb{M}_- \\ -(1-\theta)\mathbb{H}_- \end{pmatrix} \cdot \mathbf{V}_i + \begin{pmatrix} h\mathbf{F}_g \\ \mathbf{U}_{i+\theta} \end{pmatrix}, \tag{25}$$

$$\mathbf{Law}(\mathbf{U}_{i+\theta}, \mathbf{R}) = 0, \tag{26}$$

to solve over $[t_i, t_{i+1}]$, with $\mathbb{M}_\pm$ and $\mathbf{F}_g$ now meaning their global analogues, $\mathbf{V}$ and $\mathbf{R}$ contain all the degrees of freedom for all bodies (generalized velocity vector) and all the relative reactions respectively. The relative velocity $\mathbf{U}_{i+\theta}$ and $\mathbf{R}$ are conntected via some interaction law (26). Note that if Signorini non-penetration condition is used in (26), the parameter θ serves as a measure of restitution during shocks, ranging from $\theta = 0.5$(full restitution) to 1(sticking).

Global matrices $\mathbb{H}_\pm$ are comprised of $\mathbb{H}_{\alpha\pm}$ in the following way. In the beginning of each time step, the whole multi-body system is scanned for potential contact interactions. The network of contact points is only initialised for those surface FEM nodes of each solid that pass criteria of close enough proximity to another solid in the system, for the sake of decreasing the size of matrices $\mathbb{H}_\pm$. These contact points shall be called active. Matrix $\mathbb{H}_+$ is made of special block rows. The entire contact network is naturally divided into local interactions for each pair of the solids, and if a local interaction is taking place for some fixed pair of bodies l and m, this corresponds to a certain and only one block row of matrix $\mathbb{H}_+$. Each block row of such type consists of zeros and only two matrices of type $\mathbb{H}_{\alpha+}$, placed at block columns l and m. This follows from the fact that the relative velocity for two interacting solids at their common contact point α is

$$(\mathbf{U}_\alpha)_{i+1} = \mathbb{H}^l_{\alpha+}\begin{pmatrix} \mathbf{v}_C \\ \boldsymbol{\omega} \\ \boldsymbol{\lambda} \end{pmatrix}^l_{i+1} - \mathbb{H}^m_{\alpha+}\begin{pmatrix} \mathbf{v}_C \\ \boldsymbol{\omega} \\ \boldsymbol{\lambda} \end{pmatrix}^m_{i+1}$$

or with opposite sign, depending on which body is considered 'master' or 'slave' with respect to another. Note that $\mathbb{H}^l_{\alpha+}$ and $\mathbb{H}^m_{\alpha+}$ may have different number of columns, which depends on the number of Finite Element degrees of freedom each of the bodies is using, but they necessarily have the same number of rows, which is equal to 3. $\mathbb{H}_-$ is simply an explicit modification of $\mathbb{H}_+$ corresponding to orientation matrices $\mathbb{O}_i$ of each body in the network.

Schur complement system, [21], in this case is formed as

$$\begin{cases} \mathbf{U}_{i+\theta} = \mathbb{W}(\mathbf{V}_{i+1})\mathbf{R} + \mathbf{U}_{free}(\mathbf{V}_{i+1}), & \text{(27a)} \\ \mathbf{V}_{i+1} = \mathbb{B}_1(\mathbf{V}_{i+1})\mathbf{R} + \mathbf{B}_2(\mathbf{V}_{i+1}), & \text{(27b)} \end{cases}$$

where

$$\begin{aligned} \mathbb{B}_1 &= h\mathbb{M}_+^{-1}\mathbb{H}_+^T, \\ \mathbf{B}_2 &= \mathbb{M}_+^{-1}\mathbb{M}_-\mathbf{V}_i + h\mathbb{M}_+^{-1}\mathbf{F}_g, \\ \mathbb{W} &= \theta\mathbb{H}_+\mathbb{B}_1, \\ \mathbf{U}_{free} &= \theta\mathbb{H}_+\mathbf{B}_2 + (1-\theta)\mathbb{H}_-\mathbf{V}_i. \end{aligned}$$

The dependence of $\mathbb{W}$, $\mathbf{U}_{free}$ on $\mathbf{V}_{i+1}$ implies that the contact solver for (27a) must be used simultaneously along with a non-linear solver of dynamics in (27b), for example a fixed-point method. There exists a variety of contact solvers, of which the most known are the non-linear Gauss-Seidel method (NGLS) and the Newton's method, [21]. The latter is usually faster, but is not robust and may not converge for highly dynamic applications. We shall use NGLS in the numerical section due to its robustness, proven convergence results, [25]. A brief sketch of the algorithm used in the numerical section is the following.

Algorithm 1.

Necessary preprocessing and caching for all bodies, such as, for example, assembling of constant matrices and their inverse: $\mathbb{M}$, $\mathbb{K}$, $\mathbb{A}$, $\mathbf{A}$, *etc.*
Setting up initial data
while $t < T$ ***do***
  Detecting active contact points α *and assembling all* $\mathbb{C}_\alpha$
  Computing $\mathbb{H}_-$
  for $j = 1 : maxiter_1$ ***do***
    $\mathbf{R}_{prev} \leftarrow \mathbf{R}^{(j)}$
    procedure ROTATOR
      Extracting $\boldsymbol{\omega}^{(k)}$ *from* $\mathbf{V}^{(k)}$ *and updating* $\mathbb{O}_{i+1}$ *via* (24) *for each body*
      Updating $\mathbb{M}_+^{-1}$, $\mathbb{M}_+^{-1}\mathbb{M}_-$ *and* $\mathbf{F}_g$
      Updating $\mathbb{H}_+$
    end procedure
    Reassembling $\mathbb{B}_1, \mathbf{B}_2, \mathbb{W}, \mathbf{U}_{free}$
    Obtaining $\mathbf{R}^{(j)}$ *with one NLGS iteration for* (27a)
    for $k = 1 : maxiter_2$ ***do***
      $\mathbf{V}_{prev} \leftarrow \mathbf{V}^{(k)}$
      Obtaining $\mathbf{V}^{(k)} = \mathbb{B}_1\mathbf{R}^{(j)} + \mathbf{B}_2$ *for* (27b)
      if $\|\mathbf{V}^{(k)} - \mathbf{V}_{prev}\|/\|\mathbf{V}^{(k)}\| < tol_1$ ***then*** ▷ *If* $\|\mathbf{V}^{(k)}\| < \epsilon$, *use absolute error*
        break
      end if
      procedure ROTATOR
        Extracting $\boldsymbol{\omega}^{(k)}$ *from* $\mathbf{V}^{(k)}$ *and updating* $\mathbb{O}_{i+1}$ *via* (24) *for each body*
        Updating $\mathbb{M}_+^{-1}$, $\mathbb{M}_+^{-1}\mathbb{M}_-$ *and* $\mathbf{F}_g$
        Updating $\mathbb{H}_+$
      end procedure

Reassembling $\mathbb{B}_1, \mathbf{B}_2$ *only* ▷ $\mathbb{W}$ *and* $\mathbf{U}_{free}$ *only needed in the external loop*
end for
if $\|\mathbf{R}^{(j)} - \mathbf{R}_{prev}\|/\|\mathbf{R}^{(j)}\| < tol_2$ **then** ▷ *If* $\|\mathbf{R}^{(j)}\| < \epsilon$, *use absolute error*
break
end if
end for
Computing position variables $\mathbf{x}_C$, $\boldsymbol{\psi}$
$t \leftarrow t + h$
end while

Concerning implementation, note the algorithmic block called 'Rotator'. It updates all the variables for the both iterative solvers due to rotations *only*. Global mass matrices $\mathbb{M}_{\pm}$ are time-dependent only due to presence of inertia tensors $\mathbb{J}$. The inversion of $\mathbb{M}_+$ and the following multiplication $\mathbb{M}_+^{-1}\mathbb{M}_-$ for each step are computationally cheap due to block-diagonal profile of these matrices. Indeed, for an arbitrary body its inertia tensor satisfies $\mathbb{J} = \mathbb{O}\mathbb{J}_D\mathbb{O}^T$, where $\mathbb{J}_D$ is a diagonal form of the inertia tensor with respect to the floating rigid frame, so it is constant and so is its inverse. So for a single solid

$$\mathbb{J}_{i+1}^{-1} = \mathbb{O}_{i+1}\mathbb{J}_D^{-1}\mathbb{O}_{i+1}^T$$

and

$$\mathbb{J}_{i+1}^{-1}\mathbb{J}_i = \mathbb{O}_{i+1}\mathbb{J}_D^{-1}\mathbb{O}_{i+1}^T\mathbb{O}_i\mathbb{J}_D\mathbb{O}_i^T.$$

4. Numerical experiments

Three stone blocks of dimensions $1 \times 1 \times 2$ and $1 \times 0.8 \times 2$ for the upper one are placed on an absolutely rigid surface that can move along the y-axis which is initially orthogonal to the largest vertical surface of the upper block. The initial positions of center of mass are $(2/3, 0, 1)^T, (-2/3, 0, 1)^T$ and $(0, 0, 3)^T$. Refer to Fig. 2. The blocks are uniformly discretized with trilinear hexahedral element, [23], as $4 \times 4 \times 8$. There are 70 contact points in total for the simulation, 10 between each of the lower blocks and the upper one, and 25 between each of the lower blocks and the rigid surface. The Signorini velocity condition [16] and the Coulomb friction laws are used at contacts, $\theta = 1$. The friction coefficients $\mu = 0.5$ at the rigid surface and $\mu = 0.3$ between the upper block and the lower ones. The simulation was carried out with time step $h = 10^{-4}$ until $T = 1.5$, while a horizontal earthquake was imposed for the rigid surface in the direction of y axis via velocity law

$$v = \begin{cases} 0 & \text{if } t \leqslant 0.1, \\ 0.9\sin\left(\frac{5}{3}\pi(t-0.1)\right) & \text{if } t > 0.1. \end{cases}$$

The damping was added to each of the blocks in form of a matrix $\mathbb{C} = 10^{-4}\mathbb{K}$.

The main goal of the experiment was to compare the presented method of a floating frame of reference with the existing methods of small deformation and large transformation. Both latter methods were executed in open source software LMGC90. This software is based on algorithms from [18] and was designed in accordance with principles described in [26]. The Non-linear Gauss-Siedel contact solver was used in all three. The time-dependent graph of the average of the displacement over the upper block's top surface obtained from all the three methods is

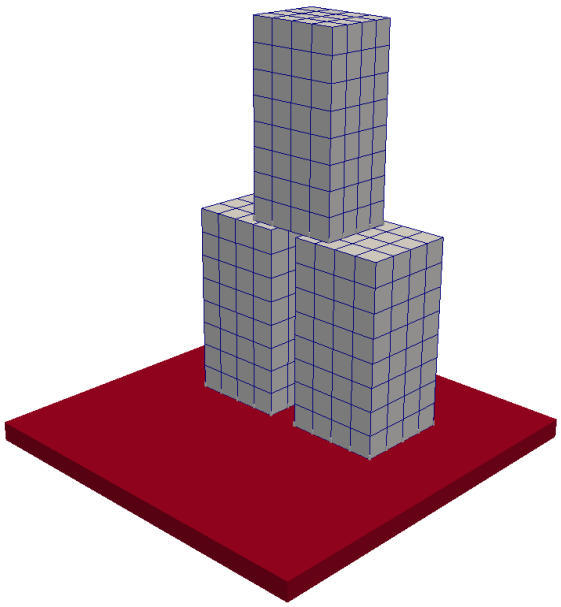

Figure 2: Blocks for simulation

shown in Fig. 3. It is clearly seen the FFR method provides much better accuracy compared to the small deformation approach which does not work reliably for finite rotations. The relative error in the displacement between curves obtained via large transformation method in LMGC90 and the FFR method is 2.1%, compared to 37.6% coming from the small deformation method. Countrary to the large transformation method, the floating frame method works more efficiently since the stiffness matrix is evaluated once in the local frame before the time evolution. In the large transformation approach, more non-linearity is added to the problem which sacrifices performance. In the presented example, the computational time for the FFR method was even reaching 2.5 times speed-up compared to the large transformation method. The tolerance of 10^{-5} was imposed for the relative error of reaction $\mathbf{R}$ in the external loop and of generalized velocity $\mathbf{V}_{i+1}$ in the internal loop of Algorithm 1. The convergence was normally being reached after 3 iterations in the internal loop and after at most 16 iterations in the NLGS in the external loop.

The method also was tested with neglect of rotational fictitious forces, i.e. term $\mathbf{F}_{rot}$ in (14). To reach the mentioned tolerance, only 2 iterations in the fixed-point loop and no more than 11 iterations in the NLGS were required. It is clearly seen that neglect of that term even for stiff solids distorts retults visibly. For better accuracy it must remain at place, although its evaluation consumes slightly more computational time. On Fig. 3, the solution curve in this case initially resembles that produced by the small deformation method.

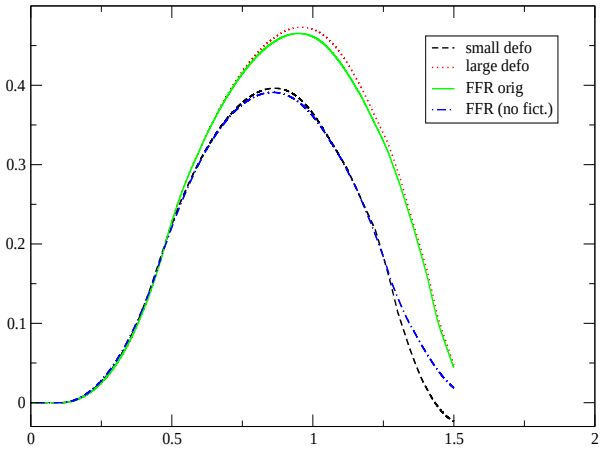

Figure 3: Mean displacement of the top surface of the upper block in the direction of earthquake

5. Conclusion

A numerical method based on the method of a floating frame of reference to solve dynamics of a system assuming small deformability and contact interactions was introduced. The main goal of the method is to conduct separation between the rigid and the deforming motions at each step by tracking the motion of the local (rigid) frame of reference and the bulk behavior of the system with respect to this frame. The method provides better experimental results for stiff systems undergoing small deformations than that provided by the method of small deformations and, compared to the large transformation approach, works faster since the linear stiffness model holds in the rigid frame.

The next step in the research would be the introduction of some mode reduction technique for the deforming part of the motion residing in the rigid frame only, in order to decrease the size of problem (25) and provide even better speed-up with insignificant sacrifice of accuracy, depending on use cases. Enrichment of the model with possibility of fracture is another direction of the research.

Appendix A.

Let D denote a determinant of the Jacobian

$$D = det\left[\frac{\partial \mathbf{x}'}{\partial \mathbf{X}}\right].$$

Then $\rho_R = \rho D$. Differentiate (6) in time. This produces two terms on the RHS, according to Leibniz's rule:

$$(\dot{\mathbb{J}\boldsymbol{\omega}}) = \int_V ((\boldsymbol{\omega} \times \mathbb{O}\mathbf{X}) \times \rho_R \mathbf{v}) dv + \int_V \mathbb{O}\mathbf{X} \times \rho_R \dot{\mathbf{v}} dv. \tag{A.1}$$

The second term on the RHS may be written for the actual domain V' and

$$\int_{V'} \mathbb{O}\mathbf{X} \times \rho \dot{\mathbf{v}} dv' = \int_V \mathbb{O}\mathbf{X} \times \mathbf{F}_{ext} D dv + \mathbb{O} \int_{V'} \mathbf{X} \times \nabla \cdot \mathbb{T} dv'.$$

Consider

$$\int_{V'} \mathbf{X} \times \nabla \cdot \mathbb{T} dv' = -\sum_{j=1}^{3} \int_{V'} \frac{\partial \mathbf{X}}{\partial x_j'} \times \mathbb{T}\mathbf{e}_j dv' + \int_{\partial V'} \mathbf{X} \times \mathbb{T}\mathbf{n} ds$$

with $\mathbf{e}_j$ meaning unit j-axis vector and $\mathbf{n}$ the outward unit normal to the surface of $\partial V'$. Linearization provides

$$-\sum_{j=1}^{3} \int_{V'} \frac{\partial \mathbf{X}}{\partial x_j'} \times \mathbb{T}\mathbf{e}_j dv' = 0, \tag{A.2}$$

and so

$$\mathbb{O} \int_{V'} \mathbf{X} \times \nabla \cdot \mathbb{T} dv' = \int_{\partial V'} \mathbb{O}\mathbf{X} \times \mathbf{R} ds. \tag{A.3}$$

It also can be shown directly that, up to linear order of bulk degrees of freedom, $D = 1 + \nabla_R \cdot \mathbf{d}'$. So we obtain

$$(\dot{\mathbb{J}\boldsymbol{\omega}}) = \int_V (1 + \nabla_R \cdot \mathbf{d}')\mathbb{O}\mathbf{X} \times \mathbf{F}_{ext} dv + \int_{\partial V'} \mathbb{O}\mathbf{X} \times \mathbf{R} ds + \mathbb{J}'\boldsymbol{\omega} \tag{A.4}$$

with tensor

$$\mathbb{J}' = \int_V \mathbb{O}\mathbf{X} \otimes \rho_R \mathbf{v}_D dv - \int_V (\mathbb{O}\mathbf{X})^T \rho_R \mathbf{v}_D dv \mathbb{I}_{3\times 3}. \tag{A.5}$$

The first term on the RHS of (A.1) is equal to $\mathbb{J}'\boldsymbol{\omega}$.

Remark 4. *Define*

$$\mathbb{G}^T = \begin{pmatrix} \int_V (\cdot) dv \\ \int_V \mathbf{r} \times (\cdot) dv \end{pmatrix}.$$

Note in case of a finite discrete mechanical system, $\mathbb{G}^T$ is a usual transposition of matrix $\mathbb{G}$. The left-hand side term of (A.2) *is a continuous analogue of the rotational part of quantity $\mathbb{G}^T\mathbf{F}_{int}$ which can be written explicitly for discrete systems. This quantity is precisely zero for purely rigid bodies, due to symmetry of the stress tensor (in the absence of force couples), and may serve as a measure of deformability of a solid.*

Acknowledgements 1. *The authors want to thank V. Acary and M. Jean for the fruitful discussions. This work has been supported by French National Research Agency (ANR) through COSINUS program (project SALADYN n°ANR-08-COSI-014).*

[1] Crisfield M (1990) A consistent corotational formulation for nonlinear three-dimensional beam elements, Comput Methods in Appl Mech and Eng 81:131-150

[2] Bergan P, Horrigmoe G (1976) Incremental variational principles and finite element models for nonlinear problems, Comp Meth in Appl Mech and Eng 7:201-217

[3] Rankin C, Brognan F (1986) An element-independent corotational procedure for the treatment of large rotations, ASME J. Pressure Vessel Technology 108:165-174

[4] Rankin C., Nour-Omid B (1988) The use of projectors to improve finite element performance, Comput Struct 30:257-267

[5] Belytschko T, Hsieh B J (1973) Nonlinear transient finite element analysis with convected coordinates, Int J Numer Meth Eng 7:255-271

[6] Simo J C (1985) A finite strain beam formulation. Part I: The three-dimensional dynamic problem, Comp Meth in Appl Mech and Eng 49:55-70

[7] Devloo P, Geradin M, Fleury R (2000) A corotational formulation for the simulation of flexible mechanisms, Multibody System Dynamics. doi: 10.1023/A:1009884131140
[8] Areias P, Garção J, Pires EB, Barbosa JI (2011) Exact corotational shell for finite strains and fracture, Comput Mech 48(4):385-406
[9] Alsafadie R, Hjiaj M, Battini J-M (2010) Corotational mixed finite element formulation for thin-walled beams with generic cross-section, Comput Methods in Appl Mech and Eng 199(49-52):3197-3212
[10] Felippa CA, Haugen B (2005) A unified formulation of small-strain corotational Finite Elements: I. Theory, Comput Methods in Appl Mech and Eng 194:2285-2335
[11] Cardona A, Geradin M (2001) Flexible multibody dynamics: a Finite Element approach, Wiley, England
[12] Veubeke BF (1976) The dynamics of flexible bodies, Int J of Eng Sci 14:895-913
[13] Shabana A, Bauchau O, Hulbert G (2007) Integration of Large Deformation Finite Element and Multibody System Algorithms, J of Comput and Nonlinear Dyn 2:351-359
[14] Banton J, Villard P, Jongmans D, Scavia C (2009) Two-dimensional discrete element models of debris avalanches: parametrisation and the reproductibility of experimental results, J of Geophys Res.-Solid Earth 114:15
[15] Manzella I, Labiouse V (2009) Flow experiments with gravels and blocks at small scale to investigate parameters and mechanisms involved in rock avalanches, Eng Geol 109:146-158
[16] Moreau JJ (1988) Unilateral contact and dry friction in finite freedom dynamics, Non-smooth Mech and Appl 302, CISM Courses and Lectures:1-82
[17] Moreau JJ (2004) An introduction to unilateral dynamics, Novel approaches in civil engineering, Lect Notes in Appl and Comput Mech 14:1-46, Springer, Berlin
[18] Jean M (1999) The non-smooth contact dynamics method, Comput Methods in Appl Mech and Eng 177:235-257
[19] Belytschko T, Liu WK, Moran B (2000) Nonlinear Finite Elements for continua and structures. Wiley, England
[20] Acary V, Brogliato B (2008) Numerical methods for nonsmooth dynamical systems; applications in mechanics and electronics, Lect Notes in Appl and Comput Mech 35, Springer, Germany
[21] Koziara T, Bicanic N (2008) Semismooth Newton method for frictional contact between pseudo-rigid bodies, Comput Methods in Appl Mech and Eng 197(33-40):2763-2777
[22] Vola D, Pratt E, Jean M, Raous M (1998) Consistent time discretization for a dynamical frictional contact problem and complementarity techniques, Rev. Europ. des Elements Finis 7:149-162
[23] Hughes TJR (1987) The Finite Element Method: linear static and dynamic Finite Element analysis. Englewood Cliffs, USA
[24] Ascher UM, Petzold LR (1998) Computer methods for ordinary differential equations and differential-algebraic equations. Society for Industrial and Applied Mathematics, USA
[25] Jourdan F, Alart P, Jean M (1998) A Gauss-Seidel like algorithm to solve frictional contact problems, Comput Methods in Appl Mech and Eng 155:31-47
[26] Dubois F, Jean M, Renouf M, Mozul R, Martin A, Bagneris M (2011) LMGC90. 10e colloque national en calcul des structures, Giens, France